An Additional H-Bond in the $\alpha_1\beta_2$ Interface as the Structural Basis for the Low Oxygen Affinity and High Cooperativity of a Novel Recombinant Hemoglobin (βL105W)†

Tsuei-Yun Fang,‡ Virgil Simplaceanu, Ching-Hsuan Tsai, Nancy T. Ho, and Chien Ho*

Department of Biological Sciences, Carnegie Mellon University, 4400 Fifth Avenue, Pittsburgh, Pennsylvania 15213

Received May 16, 2000; Revised Manuscript Received September 7, 2000

ABSTRACT: Site-directed mutagenesis has been used to construct three recombinant mutant hemoglobins (rHbs), rHb(βL105W), rHb(αD94A/βL105W), and rHb(αD94A). rHb(βL105W) is designed to form a new hydrogen bond from β105Trp to α94Asp in the $\alpha_1\beta_2$ subunit interface to lower the oxygen binding affinity by stabilizing the deoxy quaternary structure. We have found that rHb(βL105W) does indeed possess a very low oxygen affinity and maintains normal cooperativity ($P_{50} = 28.2$ mmHg, $n_{max} = 2.6$ in 0.1 M sodium phosphate at pH 7.4) compared to those of Hb A ($P_{50} = 9.9$ mmHg, $n_{max} = 3.2$ at pH 7.4). rHb(αD94A/βL105W) and rHb(αD94A) are expressed to provide evidence that rHb(βL105W) does form a new H-bond from β105Trp to α94Asp in the $\alpha_1\beta_2$ subunit interface of the deoxy quaternary structure. Our multinuclear, multidimensional nuclear magnetic resonance (NMR) studies on ^{15}N-labeled rHb(βL105W) have identified the indole nitrogen-attached ^{1}H resonance of β105Trp for rHb(βL105W). ^{1}H NMR studies on Hb A and mutant rHbs have been used to investigate the structural basis for the low O_2 affinity of rHb(βL105W). Our NMR results provide evidence that rHb(βL105W) forms a new H-bond from β105Trp to α94Asp in the $\alpha_1\beta_2$ subunit interface of the deoxy quaternary structure. The NMR results also show that these three rHbs can switch from the R quaternary structure to the T quaternary structure in their ligated state upon addition of an allosteric effector, inositol hexaphosphate. We propose that the low O_2 affinity of rHb(βL105W) is due to the formation of a new H-bond between α105Trp and α94Asp in the deoxy quaternary structure.

Human normal adult hemoglobin (Hb A),[1] the oxygen carrier within red blood cells, is a protein with a molecular weight of about 64 500, consisting of four subunits, i.e., two identical α-chains of 141 amino acids each and two identical β-chains of 146 amino acids each. Hb A is probably the most studied protein and has served as a model or paradigm for the structure−function relationship in multimeric, allosteric proteins. The oxygenation process of Hb is cooperative; i.e., the binding of the first O_2 molecule enhances the binding of the second, third, and fourth O_2 molecules. The oxygenation process is also regulated by interactions between individual amino acid residues and various solutes, known as heterotropic allosteric effectors. These effectors include ions or molecules such as hydrogen ion, chloride ion, inorganic phosphate, carbon dioxide, and organic polyanions, such as 2,3-bisphosphoglycerate (2,3-BPG) and inositol hexaphosphate (IHP). For a review on hemoglobin, see Dickerson and Geis (*1*).

The need to develop a safe, reliable blood substitute has been recognized since infections through blood transfusions with the human immunodeficiency virus that causes AIDS were reported in the mid-1980s. Also, hemoglobin-based oxygen carriers are potential sources of blood substitutes during emergency medical situations (*2*). The reasons why low O_2 affinity and high cooperativity are required for the designed Hb molecules in blood substitutes are as follows. (i) The designed Hbs should be able to deliver O_2 efficiently; i.e., they should load and unload O_2 cooperatively as Hb A does inside red blood cells. (ii) It is necessary to design Hbs with low O_2 affinity because allosteric effectors, such as 2,3-BPG, which lower the oxygen affinity of Hb within the red blood cell, are absent in the extracellular environment (*2*, *3*).

The crystal structures of Hb A in both deoxy and oxy forms (*4*, *5*), as well as the structural and functional properties of known human abnormal Hbs, can provide us with valuable information for designing novel recombinant Hbs with low O_2 affinity and high cooperativity. On the basis of a comparison of the detailed structural features of Hb A in deoxy and oxy or CO forms, Perutz and colleagues (*4*−*8*)

† This work is supported by research grants from the National Institutes of Health (R01HL-24525, R01HL-58249, and S10RR-11248).

* To whom all correspondence should be addressed: Department of Biological Sciences, Carnegie Mellon University, 4400 Fifth Ave., Pittsburgh, PA 15213. Telephone: (412) 268-3395. Fax: (412) 268-7083. E-mail: chienho@andrew.cmu.edu.

‡ Present address: Department of Food Science, National Taiwan Ocean University, Keelung, Taiwan.

[1] Abbreviations: Hb A, human normal adult hemoglobin; rHb, recombinant hemoglobin; deoxy-Hb, deoxyhemoglobin; HbO_2, oxyhemoglobin; HbCO, carbonmonoxyhemoglobin; met-Hb, methemoglobin; NMR, nuclear magnetic resonance; DSS, 2,2-dimethyl-2-silapentane-5-sulfonate; 2,3-BPG, 2,3-bisphosphoglycerate; IHP, inositol hexaphosphate; HEPES, *N*-(2-hydroxyethyl)piperazine-*N*′-2-ethanesulfonic acid; EDTA, ethylenediaminetetraacetate; 2D, two-dimensional; NOESY, nuclear Overhauser enhancement spectroscopy; HMQC, heteronuclear multiple-quantum coherence; HSQC, heteronuclear single-quantum coherence.

10.1021/bi001115i CCC: $19.00
Published on Web 10/14/2000

have shown that during the transition from the deoxy to the oxy state, the $\alpha_1\beta_2$ subunit interface undergoes a sliding movement, while the $\alpha_1\beta_1$ subunit interface remains essentially unchanged. Specific hydrogen bonds, salt bridges, and noncovalent interactions characterize both subunit interfaces. Human Hbs with mutations in the $\alpha_1\beta_2$ subunit interface are known to have altered oxygen affinity and cooperativity. It is also known that the Hb molecule has a lower O_2 affinity in the deoxy quaternary structure (T structure) than in the oxy quaternary structure (R structure) (*1*, *6*).

Proton nuclear magnetic resonance (NMR) spectroscopy has been an excellent tool for investigating the tertiary and quaternary structures of Hbs in solution (*9*). Several exchangeable proton resonances at approximately 15−9 ppm downfield from the methyl proton resonance of 2,2-dimethyl-2-silapentane (DSS) have been characterized as originating from the intersubunit H-bonds in the $\alpha_1\beta_1$ and $\alpha_1\beta_2$ subunit interfaces in both oxy and deoxy states of Hb A. These H-bonded protons observed by ^{1}H NMR can be used as structural markers in functional studies. In particular, the resonance at ∼14 ppm from DSS has been identified as the intersubunit H-bond between α42Tyr and β99Asp in the $\alpha_1\beta_2$ interface of deoxy-Hb A, a characteristic feature of the T structure of Hb A (*10*, *11*). By observing this T structure marker in both the deoxy and CO forms of Hbs under various conditions, we can assess the stability of the T conformation as well as monitor the transition from the R to the T structure.

Our strategy for designing recombinant hemoglobins (rHbs) with low oxygen affinity and high cooperativity is to stabilize the T structure while not perturbing the R structure (*3*, *12*, *13*). This strategy has been demonstrated in the design of rHb(αV96W), which has low oxygen affinity and normal cooperativity (*13*). This designed mutation is located at the $\alpha_1\beta_2$ subunit interface and in the central cavity of the Hb molecule. According to ^{1}H NMR studies, rHbCO(αV96W) can switch from the R to the T structure without changing its ligation state when the temperature is lowered and/or when IHP, an allosteric effector, is added (*13*). The crystal structure of rHb(αV96W) in the T state has shown a novel water-mediated H-bond between α96Trp Nϵ_1 and β101Glu Oϵ_2 in the $\alpha_1\beta_2$ subunit interface (*14*). Both ^{1}H NMR studies and the crystal structure indicate that the T structure of this rHb is stabilized.

In the study presented here, we have designed a mutation at position β105 to stabilize the T structure, to lower the O_2 affinity without diminishing the cooperativity, by introducing an additional H-bond into the $\alpha_1\beta_2$ subunit interface of the T structure. According to the crystal structure of deoxy-Hb-A, β105Leu is located at the $\alpha_1\beta_2$ subunit interface and is close to α94Asp at a distance of 3.5 Å (*5*). Tryptophan has been chosen to replace β105Leu due to the possibility of its forming a new H-bond with α94Asp in the T structure. The indole nitrogen-attached proton (Hϵ_1) is a good candidate for being observed by NMR, as its resonance usually occurs downfield from most other protons (*15*). Moreover, there are only three tryptophans (per αβ dimer) in the native Hb A. The oxygen-binding experiments show that this novel rHb(βL105W) does possess very low oxygen affinity and normal cooperativity. We have used both unlabeled and ^{15}N-labeled proteins to investigate the structural basis for the low O_2 affinity of rHb(βL105W) by NMR spectroscopy. We have identified the resonance of the indole nitrogen-attached proton of β105Trp for rHb(βL105W). Our NMR results also have shown that this rHb can switch from the R to the T structure without changing its ligation state when IHP is added.

To prove the formation of a new H-bond between β105Trp and α94Asp in the T structure of rHb(βL105W), two mutants, rHb(αD94A/βL105W) and rHb(αD94A), have been constructed and also studied by NMR spectroscopy. According to the crystal structure of Hb A, there is an H-bond between α94Asp and β37Trp in both the R and T structures (*4*, *5*). We expect rHb(αD94A) to lose the H-bond between residues α94 and β37 in both the R and T structures. In addition to losing the H-bond between residues α94 and β37 in both the R and T structures, rHb(αD94A/βL105W) will also lose the new H-bond between residues α94 and β105 in the T structure. In ^{1}H NMR spectra, the resonance of a proton involved in an H-bond is shifted downfield, away from the water resonance (*16*−*18*), and the magnitude of the shift correlates with the strength of the H-bond. As a corollary, we expect that when an originally H-bonded proton is no longer H-bonded, its resonance will move closer to the water resonance. Our NMR results demonstrate that rHb(βL105W) forms a new H-bond between β105Trp and α94Asp in the T structure.

MATERIALS AND METHODS

Materials. The expression vector pHE2, containing synthetic α- and β-globin genes and the *Escherichia coli* methionine aminopeptidase, was constructed in a previous study to produce authentic rHb A (*19*). The Altered Sites II *in vitro* Mutagenesis System was purchased from Promega. T4 DNA ligase, polynucleotide kinase, and restriction enzymes were obtained from Boehringer Mannheim or Promega. Synthetic oligonucleotides were obtained from DNA International. DNA sequencing was carried out at the Biotechnology Center at the University of Pittsburgh (Pittsburgh, PA). D_2O (99.9% in deuterium content) and $^{15}NH_4Cl$ (98% ^{15}N) were purchased from Cambridge Isotope Laboratories.

Site-Directed Mutagenesis. The synthetic human normal α- or β-globin gene was mutated according to the protocols of the Altered Sites II *in vitro* Mutagenesis System. The oligonucleotide primers used in site-directed mutagenesis were 5′-CTG CGT GTT GCT CCG GTC AAC TTC AAA CTG-3′ (αD94A) and 5′-G GAA AAC TTC CGA TGG CTG GGT AAC GTA C-3′ (βL105W), where the altered codons for the designed mutations are underlined. The mutated α- and/or β-globin genes were then used to replace the human normal α- and/or β-globin genes in pHE2 to construct expression vectors pHE2020, pHE2004, and pHE2017 for rHb(αD94A), rHb(βL105W), and rHb(αD94A/βL105W), respectively. The desired mutations were confirmed by DNA sequencing.

Production of Mutant rHbs. Expression vectors pHE2020, pHE2004, and pHE2017 were individually transformed into *E. coli* strain JM109. For the unlabeled rHbs, the transformed cells were grown in terrific broth (TB) medium with 100 μg/mL ampicillin at 32 °C in a 10 L Microferm fermentor (New Brunswick Scientific, model BioFlow 3000), and the production of mutant rHbs was carried out as described

previously (*19*−*21*). For the ^{15}N-labeled rHb(*β*L105W), TB medium was replaced by modified DM-1 and DM-4 media (*22*) in the seed culture and in the 5 L fermentor, respectively. In the modified DM-1 and DM-4 media, the nitrogen source was $^{15}NH_4Cl$ instead of NH_4SO_4 and yeast extract was not added.

Purification of Hb A and Mutant rHbs. Hb A was prepared and purified by standard procedures used in our laboratory (*23*). Mutant rHbs were prepared and purified as described previously (*13*, *19*−*21*, *24*, *25*).

Characterization of Mutant rHbs. N-Terminal residues were identified by Edman degradation, and molecular weights were determined by mass spectrometric analyses as in our previous studies (*13*, *19*−*21*, *24*−*26*). These two analyses were carried out to certify the quality of purified rHbs. All purified rHbs have correct molecular weights and retain less than 5% methionine at the N-termini.

Oxygen Binding of Hb Samples. The oxygen dissociation curves of Hb A and rHbs were measured with a Hemox-Analyzer (TCS Medical Products, Huntington Valley, PA) at 29 °C as previously described (*12*, *24*). The methemoglobin (met-Hb) reductase system was used if needed to reduce the amount of met-Hb in the sample (*27*). Partial oxygen pressure at 50% saturation (P_{50}) and the Hill coefficient (n_{max}) were determined from each oxygen dissociation curve [for details, see Tsai et al. (*12*)]. The accuracy for P_{50} measurements (in millimeters of mercury) is ±5%, and that for n_{max} is ±7%.

Autoxidation Measurements. The autoxidation was recorded by monitoring the rate of disappearance of the NMR oxy marker (−2.34 ppm from DSS) on a Bruker AVANCE DRX-300 spectrometer. The autoxidation reaction was carried out in PlasmaLyte buffer (Baxter) in the presence of 5% D_2O and 5 mM ethylenediaminetetraacetate (EDTA) at pH 7.4 and 37 °C. The HbO_2 concentration was 5% (∼0.8 mM).

NMR Measurements. The ^{1}H NMR experiments were performed at 29 °C on Bruker AVANCE DRX-300 and DRX-600 NMR spectrometers operating at 300.13 and 600.13 (or 600.33) MHz, respectively. Carbonmonoxy-Hb (HbCO) solutions and deoxy-Hb solutions for NMR measurements were prepared as described elsewhere (*25*). The ^{1}H NMR spectra of Hbs in H_2O were obtained by using a jump-and-return pulse sequence (*28*) with a delay time of 1.0 s. A total of 256−1024 transients were accumulated for each spectrum. Proton chemical shifts were referenced to the methyl proton resonance of 2,2-dimethyl-2-silapentane-5-sulfonate (DSS) indirectly. The water signal in samples of Hbs in H_2O (or in a 90% H_2O/10% D_2O mixture), which occurs 4.76, 4.83, and 4.92 ppm downfield from that of DSS at 29, 20, and 11 °C, respectively, was used as an internal reference. HMQC (*29*), NOESY-HMQC (*29*), and HSQC (*30*) experiments have also been performed on ^{15}N-labeled rHb(*β*L105W) and rHb A.

RESULTS

Oxygen Binding Properties of Hb A, rHb(βL105W), rHb(αD94A/βL105W), and rHb(αD94A). The oxygen binding properties of Hb A, rHb(*β*L105W), rHb(αD94A/*β*L105W), and rHb(*β*D94A) in 0.1 M sodium phosphate buffer at 29 °C are summarized in Figure 1. The effect of IHP, a strong allosteric effector, on the oxygen binding properties of rHbs is also investigated. rHb(*β*L105W) exhibits very low oxygen affinity (about 2−3 times lower) and maintains normal cooperativity from pH 7.0 to 8.0 compared to Hb A. From pH 7.4 to 8.3, rHb(αD94A/*β*L105W) and rHb(αD94A) exhibit lower oxygen affinities and almost no cooperativity compared to Hb A. The effect of pH on the oxygen affinity of Hb, the Bohr effect, can be expressed as the number of hydrogen ions released per heme upon oxygenation and can be calculated with the equation $\Delta H^+ = -\partial(\log P_{50})/\partial(\mathrm{pH})$ based on the linkage equation (*31*, *32*). The values of the Bohr effect for Hb A, rHb(*β*L105W), rHb(αD94A/*β*L105W), and rHb(αD94A) in 0.1 M sodium phosphate buffer at 29 °C are 0.61, 0.55, 0.07, and 0.11, respectively, in the pH range from pH 7.0 to 8.0. The addition of 2 mM IHP at pH ∼8.0 causes the P_{50} values to increase 165, 149, 20, and 21% for Hb A, rHb(*β*L105W), rHb(αD94A/*β*L105W), and rHb(αD94A), respectively. These results show that the Bohr effect and the IHP effect for rHb(*β*L105W) are very similar to those of Hb A. However, the Bohr effect and IHP effect for rHb(αD94A/*β*L105W) and rHb(αD94A) are quite small compared to those of Hb A. It is noted that the n_{max} value for Hb A decreases from 3.2 to 2.6 upon addition of IHP, while that for rHb(*β*L105W) decreases from 2.6 to 2.0. Additional oxygen binding experiments have been carried out to determine whether the very low oxygen affinity of rHb(*β*L105W) is caused by intrinsically low oxygen affinity in the absence of an anion or by an increased anion effect on oxygen affinity as compared to Hb A (Table 1). The intrinsic oxygen affinity of rHb(*β*L105W) is found to be about 3 times lower than that of Hb A. The cooperativity of rHb(*β*L105W) is maintained at normal values in the presence of 0, 0.01, and 0.1 M NaCl. The anion effect on the oxygen

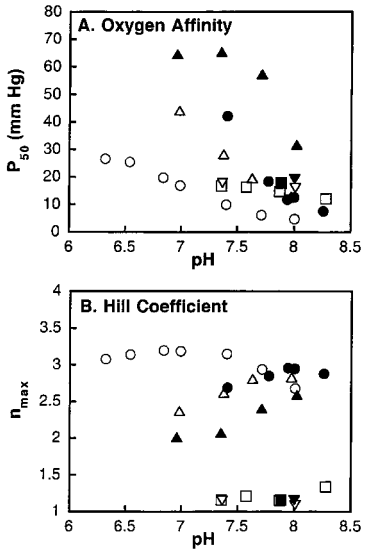

FIGURE 1: pH dependence of the oxygen affinity (A) and the Hill coefficient (B): (○ and ●) Hb A, (△ and ▲) rHb(*β*L105W), (□ and ■) rHb(αD94A), and (▽ and ▼) rHb(αD94A/*β*L105W). Open symbols depict data recorded in the absence of 2 mM IHP and filled symbols in the presence of 2 mM IHP. P_{50} and n_{max} were determined from each oxygen dissociation curve. Oxygen dissociation curves were obtained with 0.1 mM (in terms of heme) Hb in 0.1 M sodium phosphate buffer at 29 °C. The oxygen binding properties of the mutant rHbs were assessed in the presence of a reductase system (*27*) to reduce the amount of the met-Hb formed to less than 5% during the oxygenation process.

Table 1: P_{50} and n_{max} Values for Hb A and rHb(βL105W) in the Presence and Absence of NaCl[a]

	P_{50} (mmHg)			n_{max}		
	none	0.01 M NaCl	0.1 M NaCl	none	0.01 M NaCl	0.1 M NaCl
Hb A	2.8	3.3	7.3	2.3	2.6	3.1
rHb(βL105W)	9.2	10.5	18.8	2.7	2.6	2.5

[a] Data were obtained with 0.1 mM Hb in 0.1 M HEPES buffer at pH 7.4 and 29 °C.

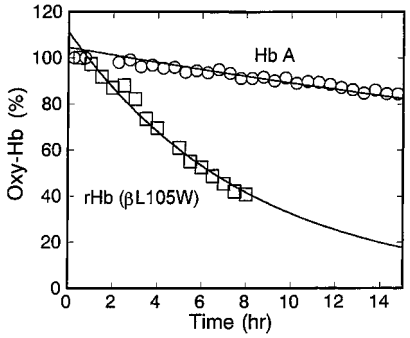

FIGURE 2: Autoxidation of (○) Hb A and (□) rHb(βL105W) in PlasmaLyte buffer in the presence of 5 mM EDTA and 5% D_2O at pH 7.4 and 37 °C. The autoxidation process was assessed by monitoring the rate of disappearance of the oxy marker at −2.34 ppm from DSS by 300-MHz ^{1}H NMR.

affinity of rHb(βL105W), however, is slightly smaller than that for Hb A.

Autoxidation Properties of rHb(βL105W). We have monitored the autoxidation process of oxy-Hb A and oxy-rHb(βL105W) by ^{1}H NMR. The resonance −2.34 ppm upfield from DSS has been assigned to the γ_2-CH_3 of E11 Val of Hb A in the oxy form (*23*, *33*). Monitoring the rate of disappearance of the oxy marker (−2.34 ppm from DSS) as a function of time allows us to determine the autoxidation rate of our Hb samples (Figure 2). The percentage of ferrous Hb varies with time (t) monoexponentially and the autoxidation rate constant can be obtained from the equation $[\text{ferrous Hb}]_t = [\text{ferrous Hb}]_{t=0} \times \exp(-k_{auto}t)$, where k_{auto} is the autoxidation rate constant. The autoxidation rate constants of Hb A and rHb(βL105W) are 0.0158 ± 0.0002 and 0.123 ± 0.0048 h^{-1}, respectively. At pH 7.4 and 37 °C in PlasmaLyte buffer, rHb(βL105W) autoxidized 8 times faster than Hb A.

^{1}H NMR Studies of the Structures of rHbs in the CO Form. ^{1}H NMR spectroscopy has been an excellent tool for investigating the tertiary and quaternary structures of Hbs (*9*). Figure 3A shows the exchangeable proton resonances of Hb A, rHb(βL105W), rHb(αD94A/βL105W), and rHb(αD94A) in the CO form. These resonances arise from the exchangeable protons in the subunit interfaces. The ^{1}H resonance at 12.8 ppm recently has been assigned to α122His in the $\alpha_1\beta_1$ interface, and the likely partner with which it forms an H-bond is β35Tyr (*34*). The resonance at 12.1 ppm was previously assigned to the H-bond between α103His and β108Asp in the $\alpha_1\beta_1$ interface (*11*). However, on the basis of our ^{1}H NMR investigation of rHb(βQ131E) (C.-K. Chang and C. Ho, unpublished results) as well as a highly refined crystal structure of deoxy-Hb A (*35*), it appears that β131Gln, not β108Asp, is the H-bond partner of α103His in the $\alpha_1\beta_1$ interfaces. Finally, on the basis of our multi-

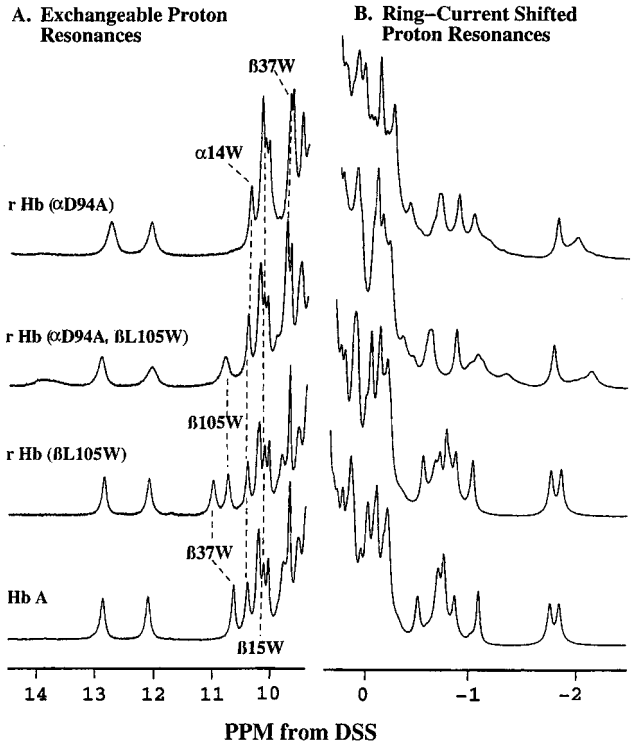

FIGURE 3: 600-MHz ^{1}H NMR spectra of 3−6% solutions of Hb A, rHb(βL105W), rHb(αD94A/βL105W), and rHb(αD94A) in the CO form in 0.1 M sodium phosphate at pH 7.0 and 29 °C: (A) exchangeable proton resonances and (B) ring current-shifted proton resonances.

nuclear, multidimensional NMR studies on ^{15}N-labeled rHb A, we have assigned the resonances at 10.6, 10.4, and 10.1 ppm to β37Trp, α14Trp, and β15Trp, respectively (*34*). These assignments indicate that the previous assignment of the resonance at 10.6 ppm to the H-bond between α94Asp and β102Asn (*10*) is incorrect.

The spectrum of rHb(βL105W) in the CO form shows an additional proton resonance in the region of exchangeable proton resonances (Figure 3A) and a shift of the resonance originally at 10.6 ppm. Since amino acid residues β37 and β105 are both located in the $\alpha_1\beta_2$ interface and are close together in the R quaternary structure (*4*), the replacement of Leu with Trp at the β105 position may cause the proton resonance of β37Trp to shift away from its original chemical shift. We have suspected that the extra resonance (at either 11.0 or 10.8 ppm) originates from β105Trp. Heteronuclear, two-dimensional (2D) NMR studies on ^{15}N-labeled rHb(βL105W) were, therefore, carried out to assign these resonances in the spectrum of rHb(βL105W) (vide infra). The spectrum of rHb(αD94A) in the CO form shows that the resonance at 10.6 ppm (assigned to β37Trp in Hb A) is missing, and a new resonance appears at 9.7 ppm compared to the spectrum of Hb A (Figure 3A, top trace). This result suggests that the shift of the resonance of β37Trp from 10.6 to 9.7 ppm (closer to the water resonance) is due to the absence of an H-bond between residues α94 and β37 in rHb(αD94A) in the CO form. This result also confirms the assignment of the resonance at 10.6 ppm to the intersubunit H-bond between α94Asp and β37Trp. The spectrum of rHb(αD94A/βL105W) in the CO form shows that one extra proton resonance appears at 10.8 ppm compared to the spectrum of rHb(αD94A). We assign the resonance at 10.8

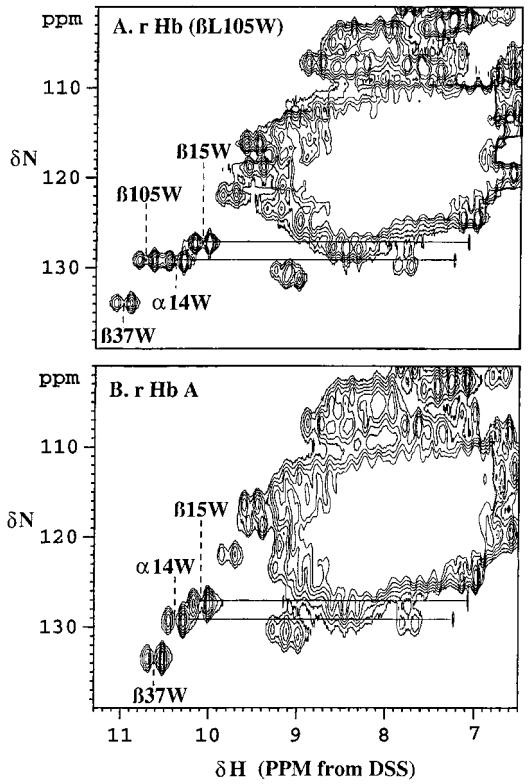

FIGURE 4: 600-MHz 2D HMQC spectra of 5−8% solutions of ^{15}N-labeled rHb(βL105W) (A) and rHb A (B) in the CO form in a 90% H_2O/10% D_2O mixture in 0.1 M sodium phosphate at pH 7.0 and 29 °C.

ppm to the indole NH of β105Trp of rHb(αD94A/βL105W) and rHb(βL105W), and then the resonance at 11.0 ppm in rHb(βL105W) is assigned to the indole NH of β37Trp.

Figure 3B shows the ring current-shifted proton resonances of Hb A, rHb(βL105W), rHb(αD94A/βL105W), and rHb(αD94A) in the CO form. The ring current-shifted resonances are very sensitive to the heme conformation and the tertiary structure of the heme pockets (*9*). The spectrum for the ring current-shifted proton resonances of rHb(βL105W) in the CO form differs only slightly from that of Hb A, while the spectra of rHb(αD94A/βL105W) and rHb(αD94A) are very different from that of Hb A. These differences imply that some adjustments of the heme conformation and/or the amino acid residues in the heme pockets have occurred due to the mutation (αD94A). Previous studies have shown that minor differences in the ring current-shifted ^{1}H resonances are common features in many mutant rHbs that we have studied (*13*, *24*−*26*). For rHb(αD94A/βL105W) and rHb(αD94A), the big differences in the ring current-shifted resonances suggest that the substitution of Ala at α94Asp causes significant changes in the conformation of the heme pockets in these two rHbs.

Heteronuclear 2D NMR Studies on ^{15}N-Labeled rHb(βL105W) in the CO Form. To assign the proton resonances at 11.0 and 10.8 ppm in the ^{1}H NMR spectrum of rHb(βL105W), heteronuclear 2D NMR studies on ^{15}N-labeled rHb(βL105W) in the CO form were performed (Figure 4 and Figure S1 in the Supporting Information). Figure 4 shows the 600-MHz HMQC spectra of ^{15}N-labeled rHb(βL105W) and rHb A in the CO form. A doublet is observed at the (^{1}Hϵ_1 and ^{15}Nϵ_1) chemical shift coordinates for Trp residues because these spectra were acquired without ^{15}N decoupling. In general, the ^{1}Hϵ_1 resonances of Trp residues usually appear at approximately 9−12 ppm (*15*, *36*) in the proton dimension, and their ^{15}Nϵ_1 resonances usually appear at approximately 121−133 ppm (*36*) in the ^{15}N dimension. The ^{15}N chemical shifts for the proton resonances at 11.0 and 10.8 ppm in the ^{1}H NMR spectrum of rHb(βL105W) are at 134 and 129 ppm, respectively, suggesting that these resonances originate from Trp residues. Since the proton chemical shift is much more easily affected by the environment than that of nitrogen, we assign 11.0 and 134 ppm to β37Trp and 10.8 and 129 ppm to β105Trp (Figure 4). This also agrees with what we observed in Figure 3A.

The HMQC spectrum also correlates the Trp ^{15}Nϵ_1 chemical shifts with the carbon-bound proton ^{1}Hδ_1 (through two-bond scalar coupling). The observation of several proton chemical shifts from the Trp indole ring protons provides additional evidence for our Trp assignments. As shown in Figure 4, we have observed the ^{1}Hδ_1 cross-peaks at 7.3 and 129 ppm and 7.1 and 127 ppm for α14Trp and β15Trp, respectively, in the spectra of both ^{15}N-labeled rHb(βL105W) and rHb A in the CO form. We also have observed the ^{1}Hδ_1 cross-peaks for β37Trp at 7.4 and 134 ppm with much weaker intensity in the spectrum of ^{15}N-labeled rHb A in the CO form (results not shown in Figure 4B). Since we have not observed the ^{1}Hδ_1 cross-peaks for β37Trp and β105Trp in the HMQC spectrum of ^{15}N-labeled rHb(βL105W) in the CO form (Figure 4A), NOESY-HMQC experiments have been performed at different mixing times to observe the ^{1}Hδ_1 and ^{1}Hζ_2 cross-peaks of all four Trp residues of rHb(βL105W) (see Figure S1 in the Supporting Information). All these results confirm the assignments for the Trp residues.

^{1}H NMR Studies of the Structures of rHbs in the Deoxy Form. Figure 5A shows the hyperfine-shifted N_δH resonances of proximal histidines in the 300-MHz spectra of Hb A, rHb(βL105W), rHb(αD94A/βL105W), and rHb(αD94A) in the deoxy form. The spectra for the hyperfine-shifted N_δH resonances of proximal histidines of the mutant rHbs in the deoxy form are very similar to that of Hb A. Figure 5B shows the hyperfine-shifted and exchangeable proton resonances in the 300-MHz NMR spectra of Hb A, rHb(βL105W), rHb(αD94A/βL105W), and rHb(αD94A) in the deoxy form. The hyperfine-shifted proton resonances arise from the protons on the heme groups and their nearby amino acid residues due to the hyperfine interactions between these protons and unpaired electrons of Fe(II) in the heme pocket (*9*). The hyperfine-shifted proton resonances in the region of 24−16 ppm are very similar between Hb A and rHb(βL105W) and are somewhat different for the other two rHbs. Figure 5C shows the exchangeable proton resonances in the 300-MHz NMR spectra of Hb A, rHb(βL105W), rHb(αD94A/βL105W), and rHb(αD94A) in the deoxy form. The ^{1}H resonance at ∼14 ppm has been identified as the intersubunit H-bond between α42Tyr and β99Asp in the $\alpha_1\beta_2$ interface in deoxy-Hb A, a characteristic feature of the deoxy T quaternary structure of Hb A (*10*, *11*). The resonance at ∼12.2 ppm has been assigned to the H-bond between α103His and β131Gln at the $\alpha_1\beta_1$ interface (C.-K. Chang and C. Ho, unpublished results). The resonance at ∼11.1 ppm has been tentatively assigned to the H-bond between α94Asp and β37Trp at the $\alpha_1\beta_2$ interface (*10*, *37*). On the basis of our recent heteronuclear, multidimensional NMR

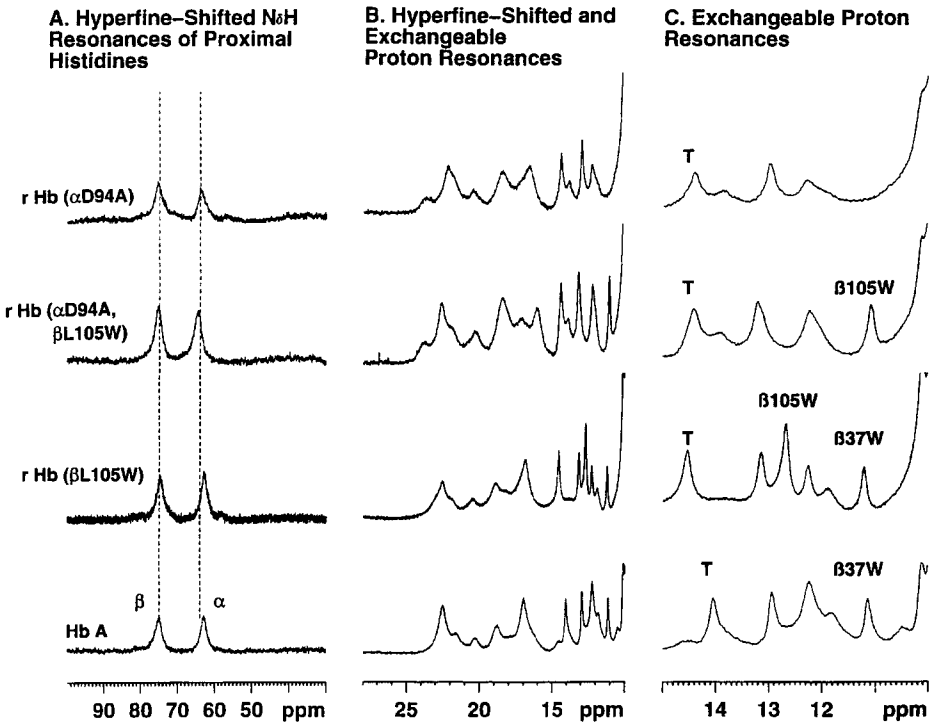

FIGURE 5: 300-MHz ^{1}H NMR spectra of 3−6% solutions of Hb A, rHb(*β*L105W), rHb(αD94A/*β*L105W), and rHb(αD94A) in the deoxy form in 0.1 M sodium phosphate at pH 7.0 and 29 °C: (A) hyperfine-shifted $N_\delta H$ resonances of proximal histidines, (B) hyperfine-shifted and exchangeable proton resonances, and (C) exchangeable proton resonances. Since rHb(αD94A/*β*L105W) and rHb(αD94A) form met-Hb during the oxygenation process, a small amount of sodium dithionite was added to these NMR samples to diminish the met-Hb.

studies on ^{15}N-labeled rHb A, we have assigned the resonance at ∼13.0 ppm to α122His, and confirmed the assignment of the resonance at ∼11.1 ppm to *β*37Trp (unpublished results). As there is no H-bond between residues α94 and *β*37 in rHb(αD94A) in the deoxy form, the resonance for *β*37Trp should shift away from its original chemical shift and closer to the water resonance (similar to what we observe in its CO form). The spectrum of rHb(αD94A) in the deoxy form does indeed show that the resonance at ∼11.1 ppm (assigned to *β*37Trp in Hb A) is missing (Figure 5C). However, we are not sure what the new chemical shift is for *β*37Trp in rHb(αD94A) in the deoxy form. The spectrum of rHb(*β*L105W) in the deoxy form shows an additional proton resonance appearing at 12.7 ppm in the region of the exchangeable proton resonances (Figure 5C). We suggest that the extra resonance at 12.7 ppm originates from *β*105Trp. The spectrum of rHb(αD94A/*β*L105W) in the deoxy form exhibits an extra proton resonance appearing at 11.1 ppm compared to that of rHb(αD94A). We suggest that this resonance originates from *β*105Trp of rHb(αD94A/*β*L105W). The NϵH resonance of *β*105Trp in rHb(*β*L105W) shifts upfield 1.7 ppm closer to the water resonance when α94Asp is replaced with Ala in rHb(αD94A/*β*L105W) (Figure 5C), consistent with the loss of H-bonding. All of these results indicate that a new H-bond forms between *β*105Trp and α94Asp in rHb(*β*L105W) in the deoxy form.

Heteronuclear 2D NMR Studies on ^{15}N-Labeled rHb(βL105W) in the Deoxy Form. To confirm the assignment of the resonance at 12.7 ppm to *β*105Trp in the ^{1}H NMR spectrum of rHb(*β*L105W) in the deoxy form, heteronuclear 2D NMR experiments on ^{15}N-labeled rHb(*β*L105W) in the deoxy form were performed (Figures 6 and Figure S2 in the Supporting Information). Figure 6 shows the 600-MHz

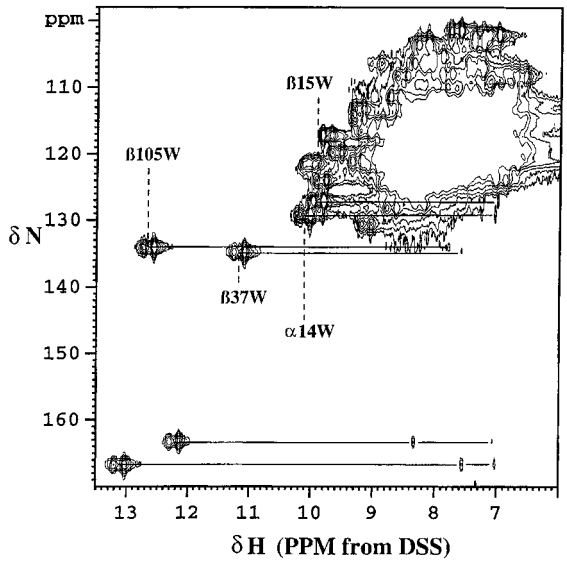

FIGURE 6: 600-MHz 2D HMQC spectrum of 5−8% solutions of ^{15}N-labeled rHb(*β*L105W) in the deoxy form in a 90% H_2O/10% D_2O mixture in 0.1 M sodium phosphate at pH 7.0 and 29 °C.

HMQC spectrum of ^{15}N-labeled rHb(*β*L105W) in the deoxy form. The ^{15}N chemical shift for the proton resonance at 12.7 ppm in the ^{1}H NMR spectrum of rHb(*β*L105W) is at 134 ppm, suggesting that this resonance originates from a tryptophan residue. In addition, we can observe the $^1H\delta_1$ cross-peaks to Trp $^{15}N\epsilon_1$ at 7.8 and 134 ppm, 7.6 and 135 ppm, 7.1 and 129 ppm, and 7.0 and 127 ppm for *β*105Trp, *β*37Trp, α14Trp, and *β*15Trp, respectively, in the HMQC spectrum of ^{15}N-labeled rHb(*β*L105W) in the deoxy form. We have also observed the $^1H\epsilon_1$ and $^1H\delta_2$ cross-peaks of His $^{15}N\epsilon_2$ for α103His at 8.3 and 163 ppm and 7.1 and 163 ppm, respectively, and for α122His at 7.6 and 167 ppm and

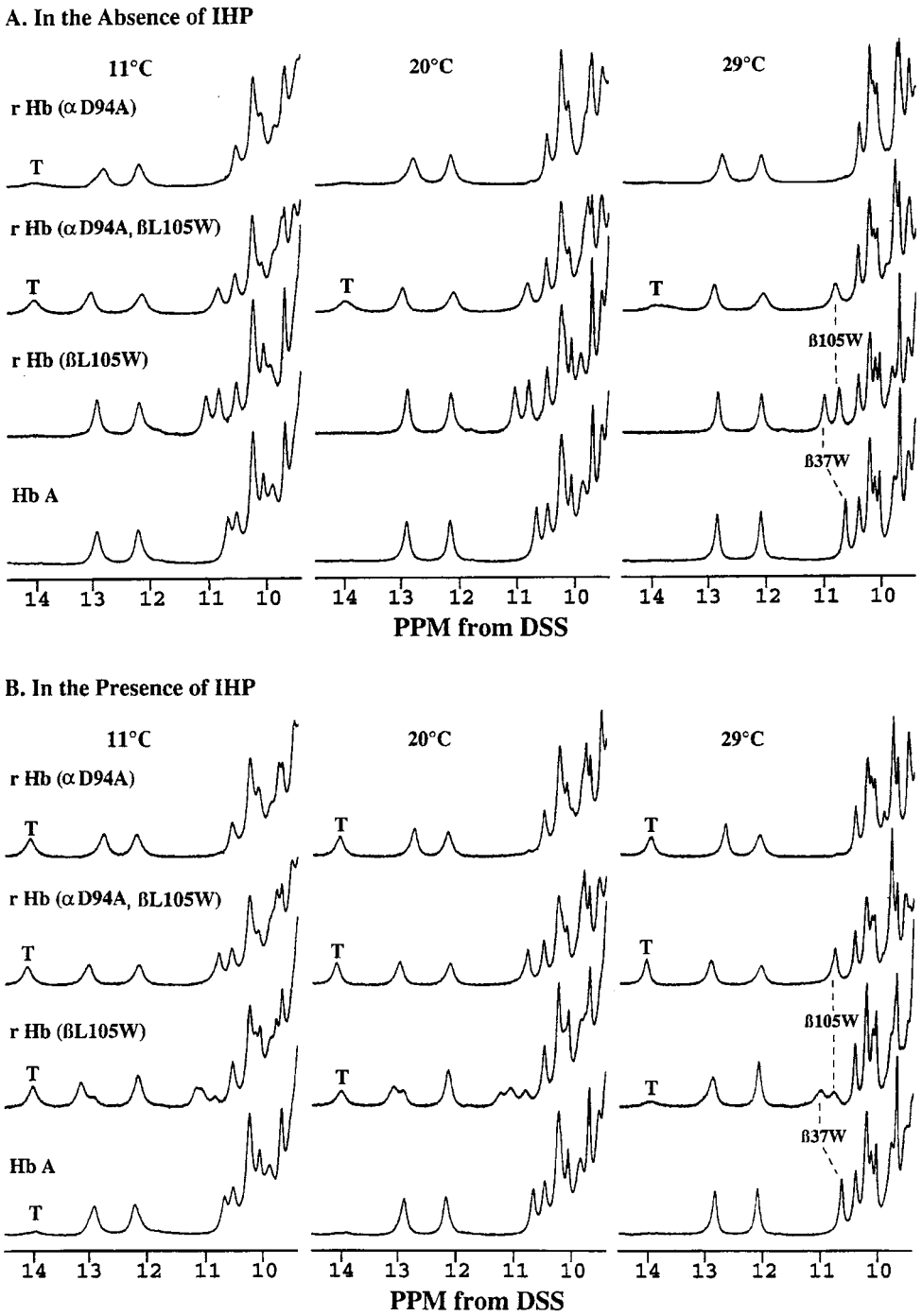

FIGURE 7: Exchangeable proton resonances in 600-MHz ^{1}H NMR spectra of 3−6% solutions of Hb A, rHb(βL105W), rHb(αD94A/βL105W), and rHb(αD94A) in the CO form in 0.1 M sodium phosphate at pH 7.0 and various temperatures in the absence (A) and presence (B) of 2 mM IHP.

7.0 and 167 ppm, respectively. NOESY-HMQC experiments have also been performed at different mixing times to provide more evidence for our assignments and to investigate the local environment of β105Trp in rHb(βL105W) in the deoxy form. For β105Trp (at 12.7 ppm), the ^{1}Hδ_1 and ^{1}Hζ_2 cross-peaks at 7.8 and 8.2 ppm, respectively, can be observed at all four mixing times (Figure S2 in the Supporting Information). For β37Trp (at 11.2 ppm), its ^{1}Hδ_1 and ^{1}Hζ_2 cross-peaks at 7.6 and 7.3 ppm, respectively, also can be observed at all four mixing times (Figure S2 in the Supporting Information). In addition, we have observed an inter-residue NOE effect between residues of β105Trp and β37Trp in the NOESY-HMQC spectra of ^{15}N-labeled rHb(βL105W) in the deoxy form as shown in Figure S2 in the Supporting Information.

Effects of IHP and Temperature on the Spectra of Hbs in the CO Form. Figure 7 shows the exchangeable proton resonances of Hb A, rHb(βL105W), rHb(αD94A/βL105W), and rHb(αD94A) in the CO form in the absence and presence of IHP at 11, 20, and 29 °C. In the absence of IHP (Figure 7A), the T marker can be observed only in the spectra of rHb(αD94A/βL105W). In the presence of IHP (Figure 7B), the T marker can be observed in the spectra of all three mutant rHbs. Besides the appearance of the T marker, the spectra of rHb(βL105W) in the CO form in the presence of IHP also show several differences compared to those in the

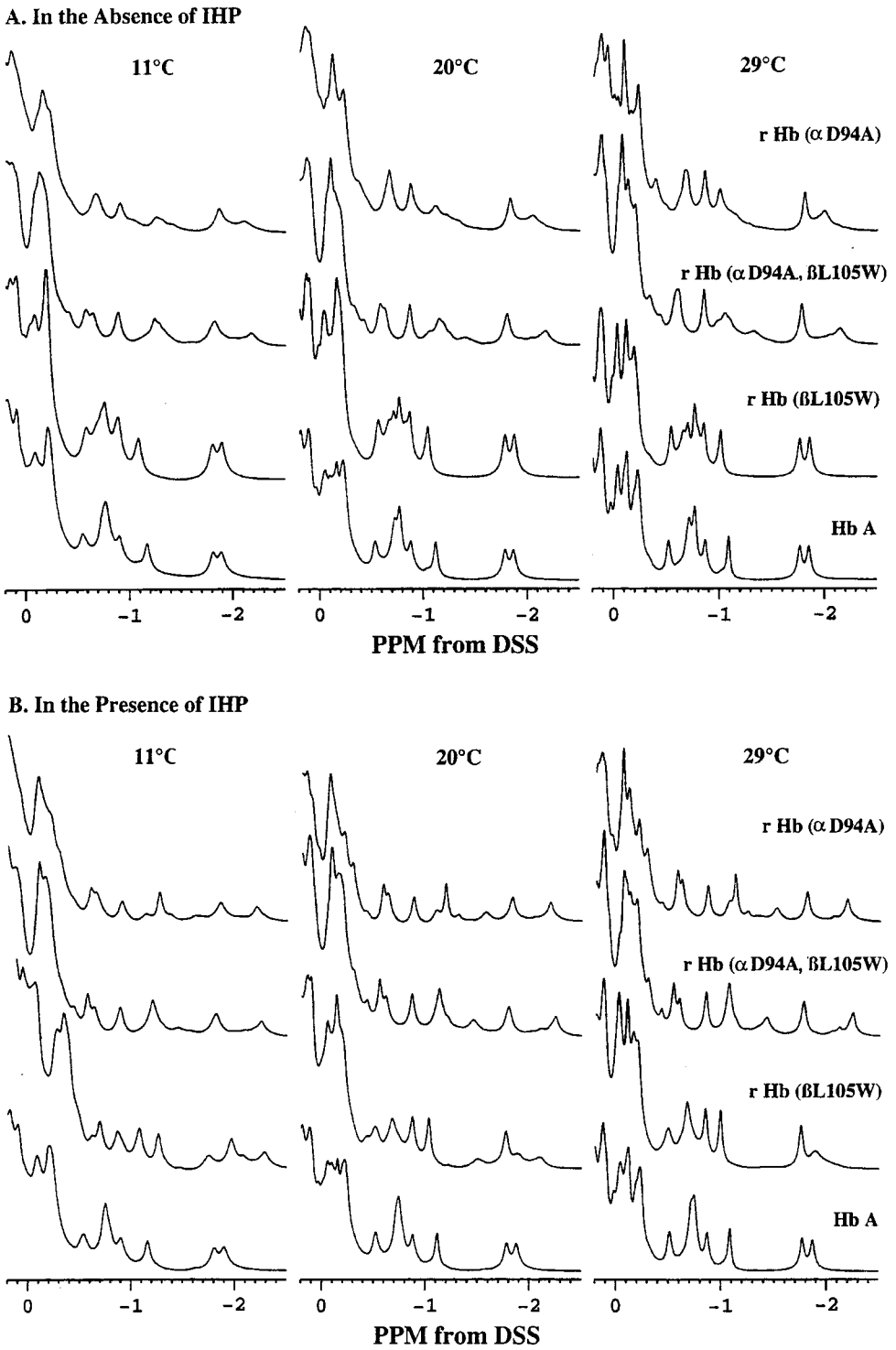

FIGURE 8: Ring current-shifted proton resonances in 600-MHz ^{1}H NMR spectra of 3−6% solutions of Hb A, rHb(βL105W), rHb(αD94A/βL105W), and rHb(αD94A) in the CO form in 0.1 M sodium phosphate at pH 7.0 and various temperatures in the absence (A) and presence (B) of 2 mM IHP.

absence of IHP (Figure 7). In the presence of IHP, new peaks at 13.1 and 11.2 ppm appear to gradually grow at the expense of the nearby resonances at 12.9 and 11.0 (or 10.8) ppm, respectively, when the temperature is lowered (Figure 7B). This suggests the existence of two conformations in slow exchange, and this conformational equilibrium is affected by a change in the temperature. To monitor these changes in more detail, HSQC experiments have been performed for ^{15}N-labeled rHb(βL105W) in the absence and presence of IHP at various temperatures (see Figure S3 in the Supporting Information). When the temperature is lowered in the presence of IHP, two new ^{1}Hϵ_1 and ^{15}Nϵ_1 cross-peaks appear at 11.0 and 131 ppm and 10.9 and 130 ppm (see Figure S3C,D in the Supporting Information). We propose that these two new cross-peaks originate from β37Trp and β105Trp in the other conformation.

Figure 8 shows the ring current-shifted proton resonances of Hb A, rHb(βL105W), rHb(αD94A/βL105W), and rHb-(αD94A) in the CO form in the absence and presence of IHP at 11, 20, and 29 °C. The ring current-shifted proton

resonances of rHb(βL105W) in the CO form differ only slightly from those of Hb A in the absence of IHP, while they are very different from those of Hb A in the presence of IHP. The ring current-shifted proton resonances of rHb(αD94A/βL105W) and rHb(αD94A) in the CO form are very different from those of Hb A in both the absence and presence of IHP, but they are very similar to each other in the presence of IHP. In addition, the ring current-shifted proton resonances of rHb(βL105W) in the CO form in the presence of IHP turn out to be somewhat similar to those of rHb(αD94A/βL105W) and rHb(αD94A) when the temperature is lowered (Figure 8B). We suspect that the spectra for the ring current-shifted proton resonances of rHb(αD94A/βL105W) and rHb(αD94A) in the CO form in the presence of IHP represent one type of spectra for rHbs in the CO form with a stable T structure. Therefore, the differences in heme pocket conformations between mutant rHbs and Hb A also suggest that these mutant rHbs switch much more easily from the R structure to the T structure, as evidenced by the appearance of the T marker in the exchangeable proton resonance region. The resonances at -1.8 and -1.9 ppm have been assigned to the heme pocket distal valine (E11) of α- and β-chains of Hb A, respectively (*33*, *38*). Compared to the spectra of Hb A, the resonance of the distal valine (E11) of the β-chain seems to be affected more in the spectra of mutant rHbs, especially in the presence of IHP, than that of the α-chain (Figure 8). These results imply that the structural switching from the R to the T structure induced by IHP, temperature, or the mutations in this study might occur mainly in the β-chain.

DISCUSSION

The $\alpha_1\beta_2$ subunit interface of Hb A is very sensitive to mutations. Most of the mutations found in the $\alpha_1\beta_2$ subunit interface region produce hemoglobins which have high oxygen affinity and very low cooperativity (*1*, *39*, *40*). However, rHb(αV96W) constructed in our laboratory (*13*) possesses low oxygen affinity (about 1.5 times lower than that of Hb A) and normal cooperativity in 0.1 M sodium phosphate from pH 6.5 to 8.0. According to the crystal structure of rHb(αV96W) in the deoxy form, there are novel water-mediated H-bonds between α96Trp and β101Glu in the $\alpha_1\beta_2$ subunit interface (*14*). Puius et al. (*14*) suggested that these novel water-mediated H-bonds in the $\alpha_1\beta_2$ subunit interface may stabilize the T structure of the protein. This example has encouraged us to design mutations located in the $\alpha_1\beta_2$ subunit interface to produce a mutant rHb which has low oxygen affinity and normal cooperativity by stabilizing the T structure without disturbing the R structure.

To lower the oxygen affinity of Hb, we have designed a mutation at residue β105 to stabilize the T structure by introducing an additional H-bond into the subunit interface of the T structure. Mutant rHb(βL105W) does possess very low oxygen affinity (3 times lower) and maintains normal cooperativity compared to that of Hb A (Figure 1 and Table 1). The normal cooperativity and the very similar spectra of rHb(βL105W) in the CO form compared to those of Hb A (Figures 3, 7A, and 8A) imply that the global R structure of rHb(βL105W) is not perturbed by the mutation. We have assigned the new resonance appearing at 12.7 ppm from DSS in the spectrum of rHb(βL105W) in the deoxy form to the new H-bond between α94Asp and β105Trp in the $\alpha_1\beta_2$ interface (Figure 5C). The appearance of the T marker in the spectra of rHb(βL105W) in the CO form also indicates that rHb(βL105W) can switch from the R to the T structure without changing its ligation state when IHP is added and the temperature is lowered (Figure 7B). These results suggest that the formation of a new H-bond between α94Asp and β105Trp in the $\alpha_1\beta_2$ interface can stabilize the T structure of this rHb. Thus, we propose that the structural basis for the low oxygen affinity of this novel rHb(βL105W) is the new H-bond formed between α94Asp and β105Trp in the $\alpha_1\beta_2$ interface in the T structure.

We propose that rHb(βL105W) has a more stable T structure than Hb A, based on the observation of the appearance of the T structural marker in the ^{1}H NMR spectra of this rHb in the CO form when the temperature is lowered and IHP is added. In other words, this rHb prefers to remain in the T quaternary structure even when it is ligated. This conclusion is supported by the following experimental results. With decreasing temperature and in the presence of IHP, rHb(βL105W) exhibits a cooperativity and oxygen affinity much lower than those of Hb A (for Hb A, $P_{50} = 10.2$ mmHg and $n_{max} = 2.5$, and for rHb(βL105W), $P_{50} = 23.5$ mmHg and $n_{max} = 2.0$, both in 0.1 M sodium phosphate and 1 mM IHP at pH 7.4 and 10 °C). It should be mentioned that rHb(αV96W/βN108K), which has the lowest oxygen affinity, exhibits the strongest T structure marker among all the low-oxygen affinity rHbs studied in our laboratory (*3*, *12*). For example, in 0.1 M phosphate and 2 mM IHP at 10 °C, rHb(αV96W/βN108K) has a P_{50} of 23.2 mmHg and an n_{max} of 1.3 (*3*). In other words, the binding of O_2 to this rHb, under these experimental conditions, is essentially noncooperative. The decreased cooperativity with decreasing temperature in the presence of IHP supports our proposal that our low-oxygen affinity rHbs prefer to remain in the deoxy state. We have observed that Hb A exhibits a 7.6-fold increase in oxygen affinity upon decreasing the temperature from 29 to 10 °C, while the oxygen affinity of rHb(βL105W) increases by only 2.5-fold. Thus, increasing the oxygen affinity upon decreasing the temperature is less pronounced in rHb(βL105W) than in Hb A, suggesting a progressive stabilization of the T structure of this mutant as the temperature is lowered. The appearance of the T state marker is an indication of a more stable T state, which serves as a molecular basis of the low oxygen affinity in rHb(βL105W).

Both rHb(αD94A) and rHb(αD94A/βL105W) have low oxygen affinities, but almost no cooperativity. These oxygen binding properties are very similar to those of human Hb mutants which have an amino acid substitution affecting the H-bond between α94Asp and β102Asn in the $\alpha_1\beta_2$ interface of the R structure, such as Hb Titusville (αD94N) (*39*) and Hb Kansas (βN102T) (*41*). Both rHb(αD94A) and rHb(αD94A/βL105W) can easily switch from the R to the T structure without changing their ligation state when IHP is added and the temperature is lowered. The replacement of Asp with Ala at the α94 position of Hb A destroys two H-bonds from α94Asp to β37Trp and to β102Asn in the $\alpha_1\beta_2$ interface of the R structure, while it destroys only one H-bond from α94Asp to β37Trp in the $\alpha_1\beta_2$ interface of the T structure. The larger disturbance produced in the R structure makes the T structure relatively more stable. Due to the mutation at residue α94, both rHb(αD94A) and rHb(αD94A/βL105W), therefore, switch more easily to the T

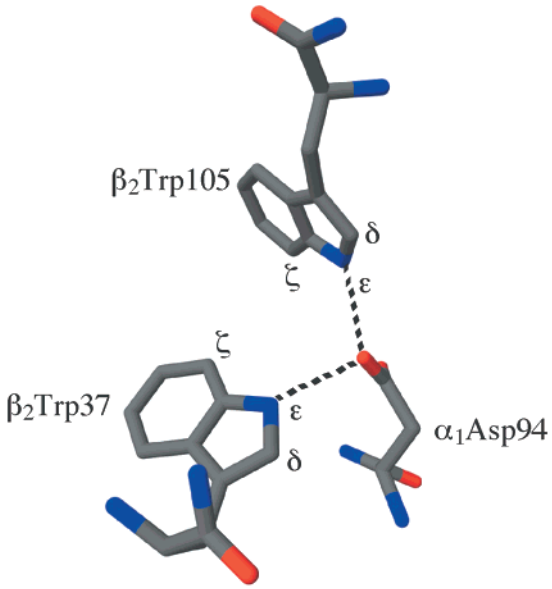

FIGURE 9: Possible geometry (or orientation) of β105Trp in rHb(βL105W) in the deoxy form. The dashed lines represent H-bonds. β105Leu has been replaced with Trp in the deoxy structure of Hb A (*5*; PDB entry 3HHB) without corrupting its nearby amino acid residues.

structure in their ligated state compared to Hb A and rHb(βL105W). Although rHb(αD94A/βL105W) switches most easily from the R to the T structure without changing its ligation state compared to other Hbs studied here, its oxygen affinity is not the lowest (see Figure 1, at pH ~7.4). This feature is different from a tendency observed from a previous study (*12*) that the rHb with the lowest oxygen affinity has the greatest tendency to switch to the T structure. We believe that the cause of rHb(αD94A) and rHb(αD94A/βL105W) not following the tendency observed from the pervious study (*12*) is that these two mutants have disturbed R structure and cannot undergo the usual T to R transition, thus exhibiting essentially no cooperativity. The disturbed R structure may also be the reason both rHb(αD94A) and rHb(αD94A/βL105W) have very small Bohr effects and small IHP effects compared to those of Hb A (Figure 1).

When we performed 2D NOESY-HMQC studies, we observed NOE effects between the side chains of β105Trp and β37Trp in the NOESY-HMQC spectra of ^{15}N-labeled rHb(βL105W) in the deoxy form (Figure S2 in the Supporting Information). Specifically, there are cross-peaks between the Hϵ_1 protons of both residues, and then cross-peaks from the Hϵ_1 of one residue to not only its own Hδ_1 and Hζ_2 but also the Hδ_1 and Hζ_2 protons of the other residue. These results indicate that residues β105Trp and β37Trp are very close in space, especially at the Nϵ_1−Cδ_1 edge, supporting the supposition that both Trp residues are involved in H-bonds to the same residue, α94Asp. Figure 9 depicts a possible geometry of β105Trp in rHb(βL105W) in the deoxy form, showing both β37Trp and β105Trp forming H-bonds with α94Asp. According to this figure, the distances from the Nϵ_1 atom of β105Trp to atoms Cδ_1 and Cζ_2 of β37Trp, from atom Nϵ_1 of β37Trp to atoms Cδ_1 and Cζ_2 of β105Trp, and from atom Nϵ_1 of β105Trp to atom Nϵ_1 of β37Trp range between 4 and 6 Å. The short distances between these atoms imply that their attached protons, Hϵ_1, Hδ_1, and Hζ_1, are very close in space. This is consistent with the fact that six inter-residue cross-peaks are observed at a mixing time of 30 ms (Figure S2 in the Supporting Information).

The ^{1}H NMR spectra of rHb(αV96W) in the CO form from a previous study (*13*) have shown that the R marker (the intersubunit H-bond between α94Asp and β37Trp) at ~10.7 ppm from DSS disappeared, while the T marker (the intersubunit H-bond between α42Tyr and β99Asp) at ~14 ppm from DSS appeared in the presence of IHP at 29 °C. A similar phenomenon has been observed for the NMR spectra of rHb(βL105W), except that the intensity of the R marker only becomes weaker (not disappearing). Interestingly, temperature-dependent ^{1}H NMR spectral changes of rHb(βL105W) in the CO form in the presence of IHP have shown that new peaks at 13.1 and 11.2 ppm gradually grow from the nearby resonances at 12.9 and 11.0 (or 10.8) ppm, respectively, when the temperature is lowered (Figure 7B). This kind of spectral change has not been observed from Hb A or other rHbs in this and previous studies (*12*, *13*). The appearance and growth of the new resonances correlate with the growth of the T marker and are indicative of a shifting equilibrium between two conformations in slow exchange. As the temperature is lowered, the T-like state becomes more populated. The exchange rate is slow on the chemical shift time scale defined by the difference in the chemical shifts of the α122His (12.9 ppm in the R state and 13.1 ppm in the T state) and β37Trp (11.0 ppm in the R state and 11.2 ppm in the T state). As the temperature is decreased, the intensity of the resonances with the chemical shift characteristic of the R state decreases, while the intensity of the resonances with the chemical shift characteristic of the T state increases. To observe both resonances, the exchange rate must be slow in comparison to that for 0.2 ppm at 600 MHz, which amounts to 120 s^{-1}.

In conclusion, the mutant rHb(βL105W) constructed in this study has further confirmed that our strategy for designing mutant Hbs with low oxygen affinity and normal cooperativity by stabilizing the T state without disturbing the R state is successful. Mutant rHb(βL105W) has very low oxygen affinity and normal cooperativity. This rHb has a more stabilized T structure based on the fact that it can switch from the R to the T structure without changing its ligation state when IHP is added. Our NMR results also suggest that rHb(βL105W) forms a new H-bond between β105Trp and α94Asp in the $\alpha_1\beta_2$ interface in the T structure. We propose that this new H-bond is the structural basis for the low oxygen affinity of rHb(βL105W).

ACKNOWLEDGMENT

We thank Dr. Ming F. Tam for carrying out N-terminal analyses by Edman degradation and electrospray ionization mass spectrometric analyses to evaluate the quality of the recombinant hemoglobins used in this study. We also thank Dr. E. Ann Pratt for helpful discussions.

SUPPORTING INFORMATION AVAILABLE

Figures S1 and S2 showing 600-MHz 2D NOESY-HMQC spectra of a 5% solution of ^{15}N-labeled rHb(βL105W) in the CO form and deoxy forms, respectively, in a 90% H_2O/10% D_2O mixture in 0.1 M sodium phosphate at pH 7.0 and 29 °C recorded at various mixing times and Figure S3 showing 600-MHz 2D HSQC spectra of 5−8% solutions of

^{15}N-labeled rHb(βL105W) in the CO form in a 90% H_2O/10% D_2O mixture in 0.1 M sodium phosphate at pH 7.0 and various temperatures in the absence and presence of 2 mM IHP. This material is available free of charge via the Internet at http://pubs.acs.org.

REFERENCES

1. Dickerson, R. E., and Geis, I. (1983) *Hemoglobin: Structure, Function, Evolution, and Pathology*, Benjamin/Cummings, Menlo Park, CA.
2. Winslow, R. M. (1992) *Hemoglobin-Based Red Cell Substitutes*, Johns Hopkins University Press, Baltimore.
3. Ho, C., Sun, D. P., Shen, T. J., Ho, N. T., Zou, M., Hu, C. K., Sun, Z. Y., and Lukin, J. A. (1998) in *Present and Future Perspectives of Blood Substitutes* (Tsuchida, E., Ed.) pp 281−296, Elsevier Science SA, Lausanne, Swizerland.
4. Shaanan, B. (1983) *J. Mol. Biol. 171*, 31−59.
5. Fermi, G., Perutz, M. F., and Shaanan, B. (1984) *J. Mol. Biol. 175*, 159−174.
6. Perutz, M. F. (1970) *Nature 228*, 726−739.
7. Baldwin, J. M., and Chothia, C. (1979) *J. Mol. Biol. 129*, 175−220.
8. Baldwin, J. M. (1980) *J. Mol. Biol. 136*, 103−128.
9. Ho, C. (1992) *Adv. Protein Chem. 43*, 153−312.
10. Fung, L. W.-M., and Ho, C. (1975) *Biochemistry 14*, 2526−2535.
11. Russu, I. M., Ho, N. T., and Ho, C. (1987) *Biochim. Biophys. Acta 914*, 40−48.
12. Tsai, C. H., Shen, T. J., Ho, N. T., and Ho, C. (1999) *Biochemistry 38*, 8751−8761.
13. Kim, H. W., Shen, T. J., Sun, D. P., Ho, N. T., Madrid, M., and Ho, C. (1995) *J. Mol. Biol. 248*, 867−882.
14. Puius, Y. A., Zou, M., Ho, N. T., Ho, C., and Almo, S. C. (1998) *Biochemistry 37*, 9258−9265.
15. Cavanagh, J., Fairbrother, W. J., Palmer, A. G., III, and Skelton, N. (1996) in *Protein NMR Spectroscopy Principles and Practice*, p 537, Academic Press, New York.
16. Llinas, M., Klein, M. P., and Neilands, J. B. (1972) *J. Mol. Biol. 68*, 265−284.
17. Wagner, G., Pardi, A., and Wuthrich, K. (1983) *J. Am. Chem. Soc. 105*, 5948−5949.
18. Redfield, A. G., and Papastratos, M. Z. (1990) *Biochemistry 29*, 3509−3514.
19. Shen, T. J., Ho, N. T., Simplaceanu, V., Zou, M., Green, B. N., Tam, M. F., and Ho, C. (1993) *Proc. Natl. Acad. Sci. U.S.A. 90*, 8108−8112.
20. Shen, T. J., Ho, N. T., Zou, M., Sun, D. P., Cottam, P. F., Simplaceanu, V., Tam, M. F., Bell, D. A., Jr., and Ho, C. (1997) *Protein Eng. 10*, 1085−1097.
21. Fang, T. Y., Zou, M., Simplaceanu, V., Ho, N. T., and Ho, C. (1999) *Biochemistry 38*, 13423−13432.
22. Looker, D., Mathews, A. J., Neway, J. O., and Stetler, G. L. (1994) *Methods Enzymol. 231*, 364−374.
23. Lindstrom, T. R., and Ho, C. (1973) *Biochemistry 12*, 134−139.
24. Kim, H. W., Shen, T. J., Sun, D. P., Ho, N. T., Madrid, M., Tam, M. F., Zou, M., Cottam, P. F., and Ho, C. (1994) *Proc. Natl. Acad. Sci. U.S.A. 91*, 11547−11551.
25. Kim, H. W., Shen, T. J., Ho, N. T., Zou, M., Tam, M. F., and Ho, C. (1996) *Biochemistry 35*, 6620−6627.
26. Sun, D. P., Zou, M., Ho, N. T., and Ho, C. (1997) *Biochemistry 36*, 6663−6673.
27. Hayashi, A., Suzuki, T., and Shih, M. (1973) *Biochim. Biophys. Acta 310*, 309−316.
28. Plateau, P., and Guéron, M. (1982) *J. Am. Chem. Soc. 104*, 7310−7311.
29. Gruschus, J. M., and Ferretti, J. A. (1998) *J. Magn. Reson. 135*, 87−92.
30. Sklenar, V., Piotto, M., Leppik, R., and Saudek, V. (1993) *J. Magn. Reson., Ser. A 102*, 241−245.
31. Wyman, J. (1948) *Adv. Protein Chem. 4*, 407−531.
32. Wyman, J. (1964) *Adv. Protein Chem. 19*, 223−286.
33. Dalvit, C., and Ho, C. (1985) *Biochemistry 24*, 3398−3407.
34. Simplaceanu, V., Lukin, J. A., Fang, T. Y., Zou, M., Ho, N. T., and Ho, C. (2000) *Biophys. J. 79*, 1146−1154.
35. Tame, J., and Vallone, B. (1998) PDB entry 1a3n.
36. BioMagResBank (1999) http://www.bmrb.wisc.edu/ref_info/statsel.html.
37. Ishimori, K., Imai, K., Miyazaki, G., Kitagawa, T., Wada, Y., Morimoto, H., and Morishima, I. (1992) *Biochemistry 31*, 3256−3264.
38. Craescu, C. T., and Mispelter, J. (1989) *Eur. J. Biochem. 181*, 87−96.
39. Schneider, R. G., Atkins, R. J., Hosty, T. S., Tomlin, G., Casey, R., Lehmann, H., Lorkin, P. A., and Nagai, K. (1975) *Biochim. Biophys. Acta 400*, 365−373.
40. Bunn, H. F., and Forget, B. G. (1986) *Hemoglobin: Molecular, Genetic, and Clinical Aspects*, Saunders, Philadelphia.
41. Bonaventura, J., and Riggs, A. (1968) *J. Biol. Chem. 243*, 980−991.

BI001115I